JACS
JOURNAL OF THE AMERICAN CHEMICAL SOCIETY

Article

pubs.acs.org/JACS

Hydrolysis of Electrolyte Cations Enhances the Electrochemical Reduction of CO_2 over Ag and Cu

Meenesh R. Singh,[†,‡] Youngkook Kwon,[†,⊥] Yanwei Lum,[†,∥] Joel W. Ager, III,[†,∥] and Alexis T. Bell*[,†,§]

[⊥]Carbon Resources Institute, Korea Research Institute of Chemical Technology, Daejeon 34114, Republic of Korea

[†]Joint Center for Artificial Photosynthesis, Material Science Division, Lawrence Berkeley National Laboratory, Berkeley, California 94720, United States

[‡]Department of Chemical Engineering, University of Illinois at Chicago, Chicago, Illinois 60607, United States

[§]Department of Chemical & Biomolecular Engineering and [∥]Department of Materials Science & Engineering, University of California—Berkeley, Berkeley, California 94720, United States

Supporting Information

ABSTRACT: Electrolyte cation size is known to influence the electrochemical reduction of CO_2 over metals; however, a satisfactory explanation for this phenomenon has not been developed. We report here that these effects can be attributed to a previously unrecognized consequence of cation hydrolysis occurring in the vicinity of the cathode. With increasing cation size, the pK_a for cation hydrolysis decreases and is sufficiently low for hydrated K^+, Rb^+, and Cs^+ to serve as buffering agents. Buffering lowers the pH near the cathode, leading to an increase in the local concentration of dissolved CO_2. The consequences of these changes are an increase in cathode activity, a decrease in Faradaic efficiencies for H_2 and CH_4, and an increase in Faradaic efficiencies for CO, C_2H_4, and C_2H_5OH, in full agreement with experimental observations for CO_2 reduction over Ag and Cu.

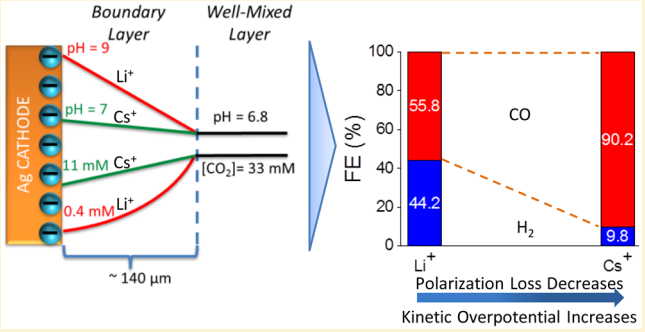

INTRODUCTION

An appealing option for the conversion of solar energy to fuels is the electrochemical reduction of CO_2 using water as the source of hydrogen.[1−3] The source of CO_2 might be the atmosphere[4] or the sea,[5] and the desired products are compounds that can be converted to a liquid using known technologies [e.g, synthesis gas (a mixture of H_2 and CO), ethene, or ethanol].[6,7] While much attention has been given to the discovery and development of catalysts, electrolytes, and electrolyte additives, these topics remain subjects of ongoing research.[8] Of the various catalysts investigated to date, Ag and Au are known to be highly selective for CO and H_2, and Cu is the metal exhibiting the highest selectivity (i.e., Faradaic efficiency) for hydrocarbons and oxygenated compounds.[9,10] Extensive work has also shown that the activity and selectivity of these catalysts can be modified by alloying,[11] surface restructuring,[12,13] surface functionalization,[14] solvent[15,16] and electrolyte composition,[17,18] and pH,[19] as well as temperature,[20] pressure,[21] and CO_2 flow rate.[9]

Recent theoretical studies have also demonstrated that the optimal bulk pH for conducting CO_2 reduction (CO2R) is close to 7 and that at significantly higher or lower values, the Nernstian losses become very high, resulting in a reduction of the total applied cell potential available to drive the kinetics of water oxidation at the anode and CO2R at the cathode.[22] It is also noted that for a bulk pH of 7, the pH of the electrolyte in the vicinity of the anode falls (i.e., the local electrolyte becomes acidic) and the pH in the vicinity of the cathode rises (i.e., the local electrolyte becomes basic) as the voltage applied across the cell increases. The latter effect is detrimental, since it results in a reduction of the dissolved CO_2 present as molecular CO_2 near the cathode and a corresponding rise in the concentration of HCO_3^- and CO_3^{2-}. The decrease in CO_2 concentration near the cathode surface leads to a reduction in the Faradaic efficiency for producing C_{2+} hydrocarbons and oxygenates and an increase in the Faradaic efficiency for producing CH_4 and H_2.[18,23]

C_{2+} products (e.g., ethene and ethanol) are preferable to C_1 products for the production of liquid fuels. However, in order to achieve the maximum selectivity to C_{2+} products and current densities of ∼10 MA cm^{-2} over Cu, the system requires potentials less than −1 V vs RHE, which results in significant polarization at the cathode.[22] Therefore, it would be desirable to find a means for offsetting the effects of electrolyte polarization occurring near the surface of the Cu cathode while a high current density and selectivity to C_{2+} products were maintained. Several investigators have shown that for a

Received: July 27, 2016
Published: September 14, 2016

DOI: 10.1021/jacs.6b07612
J. Am. Chem. Soc. 2016, 138, 13006−13012

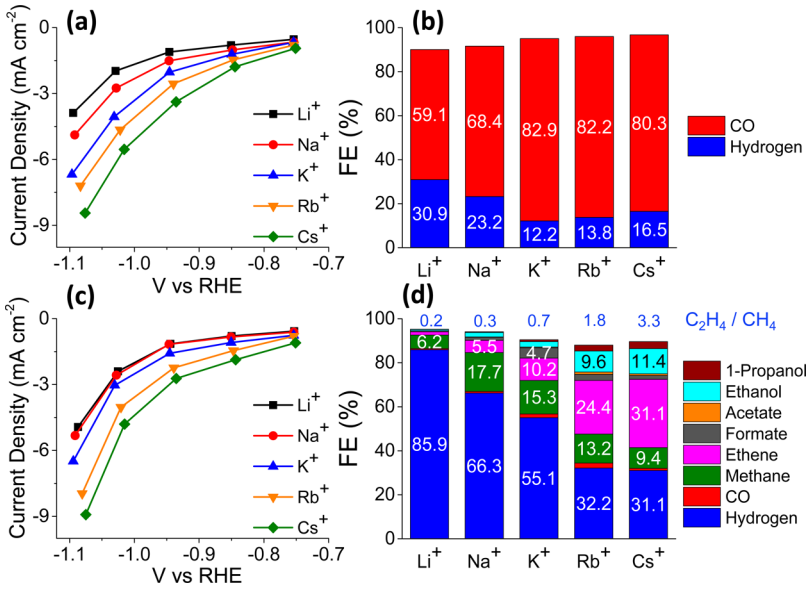

Figure 1. Influence of cation on current density and Faradaic efficiency (FE) of CO_2 reduction. (a) Current densities versus applied potential on Ag cathode, (b) FEs for CO and H_2 produced over Ag at −1 V vs RHE, (c) current density versus applied potential on Cu cathode, and (d) FEs for CO2R products produced over Cu at −1 V vs RHE in CO_2-saturated 0.1 M $MHCO_3$ (M = Li, Na, K, Rb, Cs) electrolyte. FEs for CO2R products produced over Ag and Cu at −1 V vs RHE are given in Tables S6 and S7 of the Supporting Information.

fixed applied voltage, the current density and the ratio of C_2 to C_1 products can be increased significantly by increasing the size of the alkali metal cation.[18,21,23−25] It is notable that while the effect of metal cation size on the activity of redox reactions has been known for over 45 years,[21,26] a successful interpretation of this phenomenon has not been achieved. Eyring and co-workers[21] ascribed the observation of increasing current density on Hg with increasing metal cation size to the higher specific adsorption of larger cations, the effect of which is to increase the potential of the outer Helmholtz plane (OHP) and thereby increase the kinetic overpotential at a fixed applied potential, as first proposed by Frumkin.[26] Although the effect of specific adsorption of cations provides a qualitative explanation for the increase in the total current density (i.e., activity), the increase in the selectivity of CO2R relative to that for the hydrogen evolution reaction (HER) with increasing cation size is beyond the scope of this theoretical interpretation. Murata and Hori noted the effects of cation size on the activity and selectivity to products formed during CO2R over Cu.[18] Frumkin's theory was used to explain the increase in CO2R activity, whereas the increase in the ratio of C_2 to C_1 products with increasing cation size was attributed to an increase in the equilibrium values of cathode pH with increasing OHP potential determined using the Boltzmann equation. Similar explanations for the effect of cation size on the electrochemical reduction of CO_2 have been offered by other authors.[23,24]

Recently, Janik and co-workers[27] have calculated the equilibrium potentials for cation adsorption on transition-metal electrodes and found values ranging from −2.63 V vs NHE for Li^+ to −2.44 V vs NHE for Cs^+ on Ag electrode. This suggests that the specific adsorption of cations is not favorable under operating potentials of CO2R (typically greater than −1.4 V vs NHE). Furthermore, Marković and co-workers[28] have shown that the activity of redox reactions is affected primarily by noncovalent interactions rather than covalent interactions or specific adsorption. On the basis of these findings, it is evident that Frumkin's theory of the increase in the OHP potential due to an increase in specific adsorption (or covalent interaction) of cations is not applicable to the conditions of CO2R. The steric effect due to cation size could possibly affect the OHP potential and has been investigated previously using a modified Poisson−Boltzmann equation.[29] According to predictions of this work, the variation in the size of the hydrated cation has a negligible effect on the OHP potential for the applied potentials greater than −1 V vs RHE. Therefore, it appears that neither specific adsorption nor steric hindrance of cations is responsible for the increase in the activity and selectivity reported for CO2R.

Here we report a novel interpretation of the effects of metal cation size on the electrochemical reduction of CO_2 based on preferential hydrolysis of hydrated cations near the cathode surface. We show that the pK_a for hydrolysis of hydrated cations in the bulk of the electrolyte is inversely proportional to the electrostatic energy of interaction, such that the pK_a values of Li^+ and K^+ are 13.5 and 14.6, respectively.[30,31] Under applied potential, the cations migrating toward the cathode (negative electrode) experience an increasing electrostatic interaction, which causes a decrease in the pK_a for hydrolysis. If the pK_a of the hydrated cations is lower than the local pH, the dissociation of one of the waters of hydration releases protons, thereby buffering the local pH. This effect enables the hydrated cations to buffer the electrolyte near the cathode surface, offsetting the polarization losses associated with the increase in pH, which results in a decrease in the Nernstian losses and an increase in the kinetic overpotential for a given applied voltage. Section 1 of the Supporting Information reviews the concept of metal ion hydrolysis and shows how the pK_a of hydrolysis can be calculated. The effects of cation hydrolysis on CO2R are then interpreted using a multiphysics, electrochemical model[22] presented in section 2 of the Supporting Information. This model includes the effects of ion migration, diffusion, acid−base equilibrium, gas−liquid transport of CO_2, hydrolysis of cations, and the kinetics of the OER and CO2R. The theoretical predictions are validated by comparison with the experimental measurements of CO2R over Ag and Cu electrodes using aqueous electrolytes containing alkali cations of different sizes.

DOI: 10.1021/jacs.6b07612
J. Am. Chem. Soc. 2016, 138, 13006−13012

RESULTS AND DISCUSSION

Parts a and c of Figure 1 show the cathodic current density versus voltage curves for Ag and Cu cathodes, respectively, in CO_2-saturated 0.1 M $MHCO_3$ (M = Li, Na, K, Rb, Cs) electrolytes (pH 6.8). It is evident that for a fixed potential, the current density increases 2.4-fold as the cation size increases from Li^+ to Cs^+ in the case of Ag and 2.1-fold in the case of Cu. The higher current density observed for Ag at −1 V vs RHE compared to Cu is due to the higher surface roughness of the Ag foils, which were polished mechanically, whereas the Cu foils were polished electrochemically. Figure 1a,c also shows that the electrode overpotential decreases with an increase in the cation size at a fixed current density. The influence of cation size on the Faradaic efficiencies (FEs) for CO2R products produced on Ag and Cu cathodes at −1 V vs RHE are given in parts b and d of Figure 1, respectively. The total Faradaic efficiency for CO2R over Ag and Cu cathodes increases by ∼15% and ∼55%, respectively, as the cation size increases from Li^+ to Cs^+. Figure 1d also shows that the ratio of FEs for C_2 to C_1 hydrocarbons formed over Cu increases from 0.2 for Li^+ to 3.3 for Cs^+. The measured trends of CO2R activity and selectivity are in agreement with those reported previously.[18,23,24]

To interpret the observation reported in Figure 1, we first note that the ease with which a hydrated cation undergoes hydrolysis is given by its pK_a. Table 1 shows values of the pK_a of hydrolysis for cations in the bulk electrolyte and near Ag and Cu cathode surfaces at −1 V vs RHE. It can be seen that the pK_a for cation hydrolysis in the bulk of the electrolyte increases slightly with increasing cation size due to the decrease in the electrostatic interaction between the metal cation and the O atom of a water molecule in the hydration shell. However, the pK_a near the cathode surface decreases with increasing cation size due to the increase in the electrostatic interaction between the hydrated cation and the cathode. The increase in the electrostatic interaction is due to the increase of the surface charge at a fixed solid angle on the cathode from the cation with increasing cation size (see section 1 of the Supporting Information). Therefore, the pK_a for cation hydrolysis increases monotonically with increasing separation distance between the cation and the cathode, such that it takes on the value of the bulk electrolyte for separation distances greater than ∼1 nm. As the specific capacitance and hence the charge density on the surface of Ag is higher than that on Cu, the pK_a of a cation near the Ag cathode is lower than that near the Cu cathode.

Table 1. pK_a of Hydrolysis of Cations in the Bulk Electrolyte and near Ag and Cu Cathodes at −1 V vs RHE[a]

		pK_a		
cation	cation size (pm)	in bulk electrolyte	near Ag Cathode	near Cu cathode
Li^+	69	13.6	11.64	13.16
Na^+	102	14.2	10.26	11.44
K^+	138	14.5	7.95	8.49
Rb^+	149	14.6	6.97	7.23
Cs^+	170	14.7	4.31	4.32

[a]The pK_a of hydrolysis increases linearly with the distance between the cation and the cathode. The minimum value of pK_a occurs at the cathode and the maximum value at a separation distance greater than ∼1 nm.

We have recently shown that for a near-neutral electrolyte the pH near the cathode increases during electrochemical reduction of CO_2 with increasing applied potential.[22] For example, a 0.1 M solution of $KHCO_3$ saturated with CO_2 at 1 bar has a bulk pH of 6.8 but the pH near the cathode surface can increase to as high as 9.5 for an applied potential of −1.15 V vs RHE.[22] As can be seen from Table 1, the hydrated K^+, Rb^+, and Cs^+ ions can readily undergo hydrolysis under such conditions because their pK_a values are less than 9.5, whereas Li^+ and Na^+ cations will not hydrolyze. Since the distribution of dissolved CO_2 between molecular CO_2, HCO_3^- and CO_3^{2-} is strongly dependent on pH, a high pH leads to a reduction in the concentration of molecular CO_2 due to its rapid consumption by hydroxyl anions to form HCO_3^- and CO_3^{2-}, which occurs at much higher rates than the rate of CO_2 reduction. This is detrimental to CO2R, since only molecular CO_2 undergoes reduction. A reduction in the pH near the cathode surface brought about by the buffering action of large alkali metal cations would cause the concentration of molecularly dissolved CO_2 to rise toward the value in the bulk electrolyte, 33 mM.

The effects of hydrated cation hydrolysis on CO2R over Ag and Cu cathodes were modeled using the procedures described in section 2 of the Supporting Information. Figure 2 shows calculated values of pH and CO_2 concentration at the cathode, the total current density, and FEs of CO2R products formed over Ag at −1 V vs RHE. Figure 2a shows that the cathode pH decreases from ∼9 to ∼7 with increasing cation size from Li^+ to Cs^+, in agreement with the trend in their pK_a values given in Table 1. Figure 2b shows that the cathode CO_2 concentration increases from ∼0.4 to ∼11 mM with increasing cation size. The lower concentration of CO_2 at the cathode is due to its consumption in the CO2R reaction to make products and in the acid−base equilibrium reactions to produce HCO_3^- and CO_3^{2-} anions. The CO_2 concentration is lowest at the cathode in the presence of Li^+ and Na^+ ions because the higher cathode pH >8.5 converts CO_2 to HCO_3^- and CO_3^{2-} anions. The increase in cathode pH and decrease in CO_2 concentration increase the polarization losses.[22] Therefore, the polarization losses decrease with increasing cation size. Since the applied potential is a sum of polarization loss and kinetic overpotential, the kinetic overpotential and correspondingly the current density increase with the increasing size of the cation. Figure 2c shows that the predicted current density increases with the increasing cation size, in good quantitative agreement with what is observed in Figure 1. It can be seen that the model underpredicts the current density for Li^+ and Na^+ ions and overpredicts for K^+, Rb^+, and Cs^+ ions. The difference between the predicted and measured current density can be ascribed to the direct dependence of CO_2 concentration and pH on the kinetics of CO2R, an aspect that was not considered here. For example, the increase in pH may favor electrochemical reduction of CO_2;[32] however, the decrease in CO_2 concentration will decrease the concentration of adsorbed CO_2.[9] The underestimation of the current density for Li^+ and Na^+ cations may be due to the absence of a direct dependence of pH on the kinetics of CO_2 reduction for these cations, whereas the overestimation of the current density for K^+, Rb^+, and Cs^+ cations may be due to the absence of a direct dependence of CO_2 concentration on the kinetics. Figure 2d shows that the selectivity to CO formation over Ag increases with increasing cation size. It is important to note that the HER is only affected by the polarization loss due to pH differences between the bulk

DOI: 10.1021/jacs.6b07612
J. Am. Chem. Soc. 2016, 138, 13006−13012

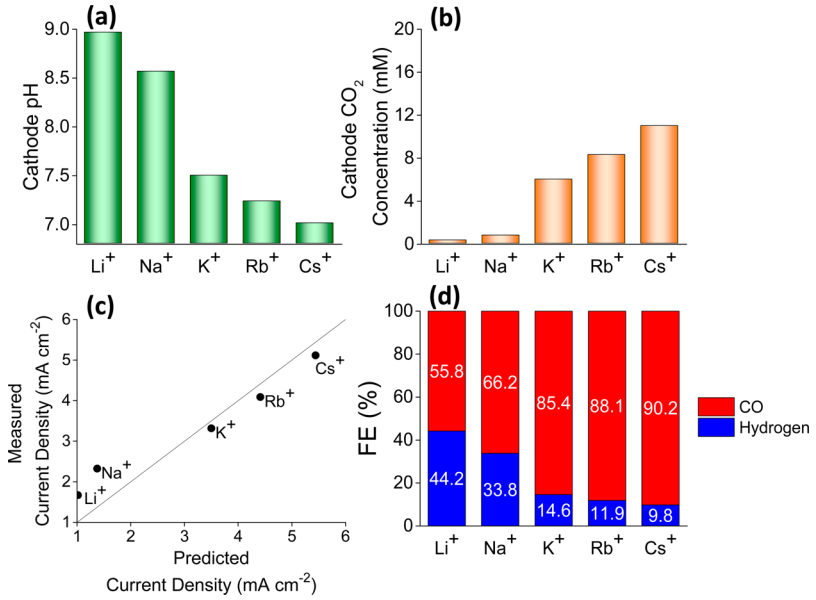

Figure 2. Calculated values of (a) cathode pH, (b) cathode CO_2 concentration, (c) total current density, and (d) Faradaic efficiencies (FEs) for CO and H_2 produced over Ag at −1 V vs RHE in CO_2-saturated 0.1 M $MHCO_3$ (M = Li, Na, K, Rb, Cs) electrolyte.

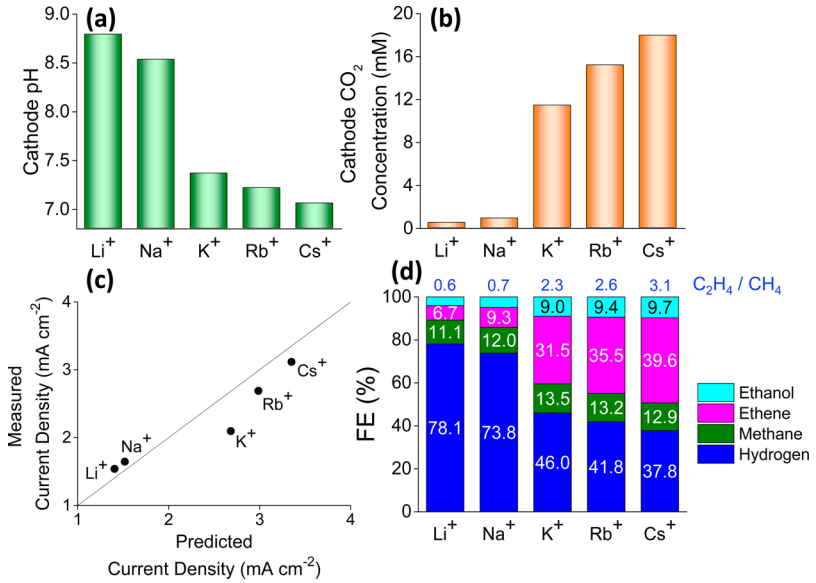

Figure 3. Calculated values of (a) cathode pH, (b) cathode CO_2 concentration, (c) total current density, and (d) Faradaic efficiencies (FEs) for C_2H_5OH, C_2H_4, CH_4, and H_2 produced over Cu at −1 V vs RHE in CO_2-saturated 0.1 M $MHCO_3$ (M = Li, Na, K, Rb, Cs) electrolyte.

and the cathode surface, whereas the CO2R reaction is affected by the polarization losses due to both pH and CO_2 concentration changes. Therefore, the current density for CO increases from 0.57 mA cm^{-2} for Li^+ to 4.9 mA cm^{-2} for Cs^+, whereas the current density for H_2 increases slightly from 0.45 mA cm^{-2} for Li^+ to 0.53 mA cm^{-2} for Cs^+. The increase in the FE for CO with increasing cation size, seen in Figure 2d, compares very well with the measured FEs presented in Figure 1b. We also notice that the FE for CO does not change significantly for bicarbonate electrolytes containing K^+, Rb^+, and Cs^+ ions, which is also explained by the model.

Figure 3 shows the influence of cation size on the calculated pH and CO_2 concentration of the electrolyte near a Cu cathode, the current density, and the FEs for CO2R products formed over Cu at −1 V vs RHE. Figure 3a shows that the cathode pH decreases from ∼8.75 to ∼7 with increasing cation size. As the current density at −1 V vs RHE on Cu is lower than on Ag, the pH near the surface of Cu is lower for a given cation than for Ag. The surface area of the Ag foils was was about 4% higher than that of the Cu foils (see Experimental Materials and Methods section), and consequently, the current density and polarization losses could be somewhat higher for Ag compared to Cu. With increasing cation size, the CO_2 concentration increases from ∼0.4 to ∼18 mM, as can be seen in Figure 3b. Since the consumption of CO_2 per electron transferred is lower for the formation of hydrocarbons than CO, the concentration of CO_2 is higher on Cu than on Ag for a given cation. As the polarization loss decreases with increasing cation size, the current density in Figure 3c increases from ∼1.5 mA cm^{-2} for Li^+ to ∼3.2 mA cm^{-2} for Cs^+. Figure 3d shows that the FEs for H_2 and CH_4 formation decrease and the FEs for C_2H_4 and C_2H_5OH formation increase with increasing cation size. The

DOI: 10.1021/jacs.6b07612
J. Am. Chem. Soc. 2016, 138, 13006−13012

polarization loss per decade change in proton and CO_2 concentrations for formation of CO is 90 mV, C_2H_4 is 70 mV, C_2H_5OH is 70 mV, CH_4 is 67.5 mV, and H_2 is 60 mV. The sensitivity of current density with respect to polarization losses depends on the transfer coefficient of the reaction. Table S5 in the Supporting Information shows that the experimentally measured transfer coefficients decrease in the order C_2H_4 > C_2H_5OH > $CH_4 \gg H_2$. Therefore, the partial current density of C_2H_4 and C_2H_5OH increases significantly as compared to that for CH_4 and H_2 with increasing cation size, resulting in an increase in the FEs for C_2 hydrocarbons products but a decrease in the FEs for CH_4 and H_2. The predicted ratio of the selectivity of C_2 to C_1 hydrocarbons increases from 0.6 for Li^+ to 3.1 for Cs^+ and agrees well with the experimental values in Figure 1d.

The quantitative agreement between the theoretical predictions and the experimental measurements confirms that the variation in the activity and selectivity of CO2R reactions with the cation size is due to the buffering ability of the cations in the vicinity of the cathode. The proposed effect of hydrolysis of hydrated cation is a macroscopic phenomenon that is effectively captured by our continuum model. The local buffering capability of cations should be able to increase the rate of any proton-transfer reaction. In section 3 of the Supporting Information we show that the current density for HER on a Ag cathode at −1 V vs RHE in 0.1 M chloride increases from ∼2.5 mA cm^{-2} for Li^+ to ∼4.5 mA cm^{-2} for Cs^+. The differences between the HER current densities for different cations increase with increasing applied potential as a consequence of increasing buffering at higher applied voltages. As the polarization loss is negligible at −0.7 V vs RHE, the current density for HER does not change with cation size. It is, therefore, evident that larger cations promote not only CO2R but also HER.

For a given cation, the electrode charge density can be manipulated to control the pK_a of hydrolysis. The surface charge density of the electrode at a fixed cathode potential can be increased by increasing the total cell voltage, for example, by using a high overpotential anode and a large gap between the electrodes. While this strategy would lower the electrolysis efficiency, it would increase the CO2R activity and selectivity. The hydrated cations can promote proton transfer only when (i) the electrolyte is neither strongly acidic nor alkaline and (ii) the pK_a of hydrolysis is close to the local electrolyte pH. In this connection, we note that the pH near the electrode surface does not change significantly with the applied voltage in strongly alkaline medium. Since the pK_a values for different cations are typically less than 13, the buffering capacities of these cations are similar under alkaline conditions. Therefore, the polarization losses and thereby the kinetic overpotentials at a fixed applied potential are the same for different cations. In agreement with this effect, Figure S5 in the Supporting Information shows that the selectivity and activity for CO reduction over Cu at −1 V vs RHE in pH 13 electrolytes do not change significantly with cation size.

CONCLUSION

The effects of cation size on the electrochemical reduction of CO_2 over catalysts such as Hg, Ag, and Cu have been reported in a number of studies over the past 45 years. Attempts to explain this phenomenon have focused on specific adsorption and steric hindrance of cations in the inner and outer Helmholtz planes, respectively. However, recent calculations have raised questions about the validity of these explanations, since neither specific adsorption nor steric hindrance of cations is possible under the operating conditions used for CO2R. In this study, we present an interpretation of the effects of electrolyte cations on the electrochemical reduction of CO_2 over Ag and Cu. The essence of our findings is summarized in Figure 4. We show that the hydrated alkali metal cations in the bulk of the electrolyte are stable to hydrolysis but can undergo hydrolysis in proximity to the cathode as a consequence of Coulombic interactions with the negative charge on the cathode, an effect that increases linearly with increasing cathode potential. The hydrated cations act as a pH buffer near the cathode. As discussed in section 2 of the Supporting Information, the pK_a of the hydrated cations is determined by the charge and size of cation and the charge density on the cathode. The pK_a of cations near a cathode maintained at −1 V vs RHE decreases with increasing cation size, and consequently, the buffering capability decreases in the order $Cs^+ > Rb^+ > K^+ > Na^+ > Li^+$. Consequently, the pH decreases and the CO_2 concentration increases near the cathode with increasing cation size. The resulting polarization losses at the cathode causes the FEs for H_2 and CH_4 to decrease and the FEs for CO, C_2H_4, and C_2H_5OH to increase with increasing cation size. The proposed interpretation gives satisfactory quantitative agreement between experimental observations and theoretical predictions at −1.1 V vs RHE.

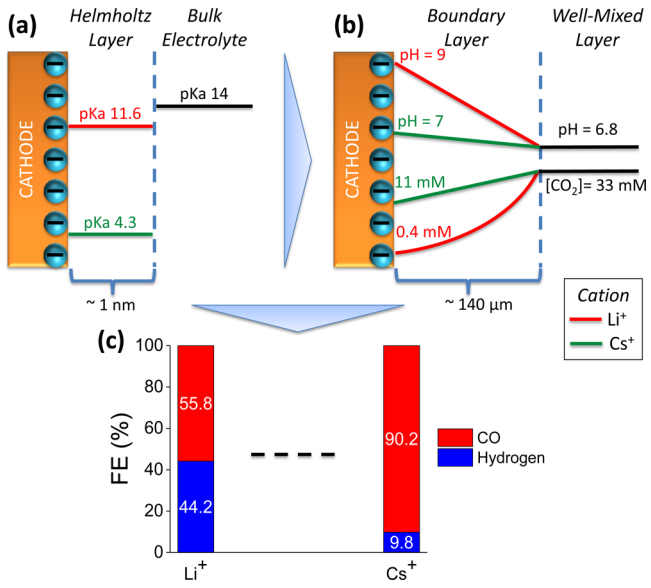

Figure 4. Effect of cation hydrolysis on the electrochemical reduction of CO_2 over Ag. (a) pK_a of hydrolysis of hydrated Li^+ and Cs^+ inside the Helmholtz layer and in the bulk electrolyte and (b) distribution of pH and CO_2 concentration in the boundary layer. Hydrated Cs^+ buffers the cathode to maintain the pH close to 7 and to increase the CO_2 concentration, whereas hydrated Li^+ does not buffer the cathode, which leads to an increase in the pH to 9 and a decrease in CO_2 concentration to 0.4 mM. (c) FE for CO increases and for H_2 decreases with increasing cation size due to a decrease in polarization.

At less negative applied voltages, the pH of the electrolyte near the cathode rapidly falls to that of the bulk solution and the predicted pK_a of hydrolysis becomes that of the bulk electrolyte, pH 6.8. For instance, at −0.7 V vs RHE, the pK_a of Li^+ is 14.4, Na^+ is 13.6, K^+ is 12.3, Rb^+ is 11.8, and Cs^+ is 10.9 over Cu. Therefore, the cations will not undergo hydrolysis at

DOI: 10.1021/jacs.6b07612
J. Am. Chem. Soc. 2016, 138, 13006−13012

voltages more positive than −0.7 V vs RHE. We note, however, that our experimental results show that the nature of the cation also affects the current densities at low applied voltages. This effect cannot be attributed to hydrolysis of the hydrated cations near the cathode nor, as explained in the Introduction, to the specific absorption or steric hindrance of cations. It may, instead, be due to the influence of cations in stabilizing the adsorption of CO_2 at the cathode; however, this effect would need to be very strong in order to offset the very low concentration of cations relative to Ag sites at the cathode surface. Further research work is required to identify the effects of the nature of cations on the current density and the distribution of products observed at applied voltages greater than −0.7 V. For applied voltages less than −0.8 V, the effect of polarization losses is to shift the polarization curves shown in Figure 1a,c toward more negative voltages. It is possible to plot the partial current densities against the applied potential corrected for the polarization losses (equivalently, kinetic overpotential), which should make all plots for different cations collapse into a single plot representing the intrinsic kinetics of the CO_2 reduction reaction.

It is noted that the hydrolysis of hydrated cations can be effective only if (i) the electrolytes are neither strongly acidic nor alkaline and (ii) the pK_a for hydrolysis of the hydrated cation is close to the local pH of the electrolyte, and this effect will be strongest for systems in which the local concentration of the reactant (e.g., CO_2) is pH-dependent. The present study further reveals that hydrolysis of hydrated cations can be used to increase the activity and selectivity of any proton-transfer reaction on any conductive electrode. Our model can be applied to any electrode for which the reaction kinetics and specific capacitance are known. The specific capacitance is used to determine the pK_a for cation hydrolysis, and the kinetics are needed to specify the boundary conditions for the transport equations. On the basis of the concept of hydrolysis, several practical strategies can be employed to increase electrocatalytic activity and selectivity by (i) increasing the local concentration of cations by tethering or physically coating anionic ionomers on the cathode, (ii) decreasing the pK_a of hydrolysis by increasing the cell resistance or capacitance, and (iii) using multivalent cations.[33] The pK_a of multivalent cations can be computed using eq 4 of the Supporting Information, provided that the electronegativity of cations is <1.5, which is true for alkali metal and alkali earth cations. The hydrolysis of multivalent cations can be included in the transport equations in a similar manner to that shown for monovalent cations in the Supporting Information. The multivalent cations are better for CO2R than the monovalent cations, as the higher positive charge on the multivalent cations increases the polarity of the OH bond in the waters of the hydration shell, which makes them easier to hydrolyze. However, their application in electrolysis is limited due to their lower solubility in aqueous solutions.

METHODS

Experimental Materials and Methods. *Materials.* Lithium carbonate (≥99.998% metals basis), sodium carbonate (≥99.9999% metals basis), potassium carbonate (≥99.995% metals basis), rubidium carbonate (≥99.8% metals basis), cesium carbonate (≥99.995% metals basis), lithium chloride (99.998% metals basis), sodium chloride (99.999% metals basis), potassium chloride (99.999% metals basis), rubidium chloride (≥99.95% metals basis), cesium chloride (≥99.999% metals basis), lithium hydroxide (99.95% metals basis), sodium hydroxide (99.99% metals basis), potassium hydroxide (99.99% metals basis), rubidium hydroxide solution (99.9% metals basis), and cesium hydroxide (99.95% metals basis) were purchased from Sigma-Aldrich. Copper foil (99.9999% metals basis, 0.1 mm thickness) and silver foil (99.998% metals basis, 0.25 mm thickness) were purchased from Alfa Aesar. Water-based alumina fine polishing suspension (0.05−0.3 μm) and polishing cloth (Alpha-A, 8″) were purchased from Ted Pella, Inc. Carbon dioxide (99.995%), nitrogen (99.999%), helium (99.999%), and hydrogen (99.999%) were purchased from Praxair. Hydrogen, helium, nitrogen, and carbon dioxide gas purifiers were purchased from Valco Instruments Co. Inc. Electrolyte solutions were prepared with 18.2 MΩ deionized (DI) water obtained from a Millipore system.

Electrode and Electrolyte Preparation. Copper and silver foils were cut into electrodes of 2 × 2 cm^2 squares and then cleaned by sonicating for 30 min in acetone, followed by 2-propanol and finally deionized (DI) water. Cu foil was electropolished in concentrated phosphoric acid at a potential of 2.0 V for 5 min with a copper foil counter electrode, followed by rising with DI water and drying with a stream of nitrogen. As Ag oxidizes during electropolishing to form a layer of AgO, we chose to mechanically polish Ag foils. Ag foil was polished mechanically using an alumina suspension down to 0.05 μm on a polishing cloth, then sonicated and rinsed with DI water, and dried under nitrogen. As a result of the different electrode polishing procedures, the macroscopic roughness measured using AFM was 1.0400 for Ag foil and 1.0001 for Cu foil. To prepare 0.1 M of bicarbonate solution, 0.05 M of carbonate solution was sparged for 1 h with a flow of pure CO_2 at 1 bar.

Electrochemical Measurements. Electrochemical measurements were carried out using a Biologic SP-300 potentiostat. Ambient pressure CO_2/CO electrolysis was carried out in a custom-made gastight electrochemical cell. In brief, the working electrode is parallel to the counter electrode in order to ensure a uniform potential distribution across the surface. The geometric surface area for both of the electrodes is 1 cm^2, the volume of the anolyte and catholyte are 1.3 mL each, and the headspace volume is approximately 3 mL. A Selemion AMV anion-exchange membrane was used to separate the anodic and cathodic compartments. Before conducting CO_2/CO electrolysis, the electrolyte was purged with CO_2/CO for at least 15 min to achieve an electrolyte pH of 6.8, thereby ensuring that the solution was CO_2/CO saturated. During electrolysis, CO_2/CO was constantly bubbled through the electrolyte at a flow rate of 5 sccm to prevent depletion of CO_2/CO and to ensure a constant flow of gas through the gas chromatograph. The flow rate of CO_2/CO was controlled with a mass flow controller (MKS Instrument). For all experiments, platinum foil was used as the counter electrode and Ag/AgCl electrode (leak free series) from Innovative Instruments, Inc., was used as the reference. Data were converted to the RHE reference scale using the equation:

$$E(\text{vs RHE}) = E(\text{vs Ag/AgCl}) + 0.197\ \text{V} + 0.0591 \times \text{pH}$$

where the pH was 6.8. To ensure the accuracy of the reference electrodes, calibration was done with a homemade reversible hydrogen electrode. Potentiostatic electrochemical impedance spectroscopy (PEIS) was used to determine the total uncompensated resistance (R_u) by applying frequencies from 10 Hz to 30 kHz at the open circuit potential. The potentiostat compensated for 85% of R_u in situ, and the last 15% was postcorrected to arrive at accurate potentials.

HER Measurements with Silver. The exact same electrochemical cell as the one utilized for CO2R was employed. However, in this case, Ar was continuously bubbled through at a flow rate of 5 sccm to create an inert environment. Also, 0.1 M chloride solutions of the different cations were used as the electrolyte. Chronoamperometry was carried out to determine the current density for hydrogen evolution on a polycrystalline silver foil as a function of potential. The potential was stepped at 3 min intervals to various potentials. The current density at a specific potential was calculated as the average value during the 3 min interval.

Product Analysis. A gas chromatograph (Agilent Technologies) equipped with a packed HaySep Q column and a carbon column was used for analysis of gaseous products. H_2, CO, CH_4, C_2H_4, and C_2H_6

DOI: 10.1021/jacs.6b07612
J. Am. Chem. Soc. 2016, 138, 13006−13012

were detected by a pulsed-discharge, helium ionization detector (PDHID). Calibration of the gas chromatograph was carried out using calibration gas prepared by Praxair (UN 1956). During electrolysis, CO_2/CO was allowed to flow from the electrochemical cell directly into the gas sampling loop of a gas chromatograph for online gaseous product analysis, which was carried out every 25 min. For all experiments, electrolysis was allowed to proceed for 1.5 h with gas analysis done at the 10, 35, 60, and 85 min.

Liquid products were collected from the cathode and anode chambers after electrolysis and analyzed by high-performance liquid chromatography (HPLC) on an UltiMate 3000 HPLC (Thermo Scientific). Vials containing liquid samples were placed in an autosampler holder, and 10 μL of sample was injected into the column. The column used was an Aminex HPX 87-H (Bio-Rad), and diluted sulfuric acid (1 mM) was used as the eluent. The temperature of the column was maintained at 60 °C in a column oven, and the separated compounds were detected with a refractive index detector (RID). The expected products of CO2R were analyzed as well by HPLC to produce a standard calibration curve at 60 °C (i.e., formate, acetate, ethylene glycol, ethanol, and *n*-propanol).

Double-Layer Capacitance Measurements. The double-layer capacitance values were measured utilizing methods described by Kanan and co-workers.[13] In brief, this was done by performing cyclic voltammetry in a non-Faradaic potential regime. The exact same electrochemical cell as the one utilized for CO2R was employed. In this case, a Nafion proton exchange membrane was used and 0.1 M $HClO_4$ was used as the electrolyte. Cyclic voltammetry was performed with different scan rates and the geometric current density was plotted against the scan rate. The double layer capacitance was determined by calculating the slope of this graph.

Computational Methods. The mathematical model for the electrochemical cell previously developed by Singh et al.[22] was used to analyze the effects of cation size on the overall activity and selectivity of Ag and Cu cathodes. A synopsis of the model is given in section 2 of the Supporting Information. The mathematical model was solved using COMSOL Multiphysics 4.3b to obtain product current densities at −1 V vs RHE in 0.1 M $MHCO_3$ electrolyte.

■ ASSOCIATED CONTENT

Supporting Information

The Supporting Information is available free of charge on the ACS Publications website at DOI: 10.1021/jacs.6b07612.

Theory of hydration and hydrolysis of metal ions, prediction of partial current density, effect of cations on the hydrogen evolution reaction at neutral pH, effect of cations on the CO reduction reaction in alkaline electrolyte, effect of cation on the Faradaic efficiency for CO2R products produced over Ag and Cu at −1 V vs RHE, Tables S1−S7, and Figures S1−S4 (PDF)

■ AUTHOR INFORMATION

Corresponding Author

*alexbell@berkeley.edu

Author Contributions

M.R.S, Y.K, and Y.L. contributed equally to this work.

Notes

The authors declare no competing financial interest.

■ ACKNOWLEDGMENTS

This material is based on the work performed by the Joint Center for Artificial Photosynthesis, a DOE Energy Innovation Hub, supported through the Office of Science of the U.S. Department of Energy under Award number DE-SC0004993. Y.L. acknowledges the support of an A*STAR National Science Scholarship.

■ REFERENCES

(1) Singh, M. R.; Clark, E. L.; Bell, A. T. *Proc. Natl. Acad. Sci. U. S. A.* **2015**, *112*, E6111.
(2) Chu, S.; Majumdar, A. *Nature* **2012**, *488*, 294.
(3) Graves, C.; Ebbesen, S. D.; Mogensen, M.; Lackner, K. S. *Renewable Sustainable Energy Rev.* **2011**, *15*, 1.
(4) Goeppert, A.; Czaun, M.; Prakash, G. K. S.; Olah, G. A. *Energy Environ. Sci.* **2012**, *5*, 7833.
(5) Eisaman, M. D.; Parajuly, K.; Tuganov, A.; Eldershaw, C.; Chang, N.; Littau, K. A. *Energy Environ. Sci.* **2012**, *5*, 7346.
(6) Heveling, J.; van der Beek, A.; de Pender, M. *Appl. Catal.* **1988**, *42*, 325.
(7) Narula, C. K.; Davison, B. H. U.S. Patent No. 9,181,493, 2014.
(8) Costentin, C.; Robert, M.; Savéant, J.-M. *Chem. Soc. Rev.* **2013**, *42*, 2423.
(9) Hatsukade, T.; Kuhl, K. P.; Cave, E. R.; Abram, D. N.; Jaramillo, T. F. *Phys. Chem. Chem. Phys.* **2014**, *16*, 13814.
(10) Clark, E. L.; Singh, M. R.; Kwon, Y.; Bell, A. T. *Anal. Chem.* **2015**, *87*, 8013.
(11) Kim, D.; Resasco, J.; Yu, Y.; Asiri, A. M.; Yang, P. *Nat. Commun.* **2014**, *5*, 4948.
(12) Lu, Q.; Rosen, J.; Zhou, Y.; Hutchings, G. S.; Kimmel, Y. C.; Chen, J. G.; Jiao, F. *Nat. Commun.* **2014**, *5*, 3242.
(13) Li, C. W.; Ciston, J.; Kanan, M. W. *Nature* **2014**, *508*, 504.
(14) Tripkovic, V.; Vanin, M.; Karamad, M.; Björketun, M. r. E.; Jacobsen, K. W.; Thygesen, K. S.; Rossmeisl, J. *J. Phys. Chem. C* **2013**, *117*, 9187.
(15) Kaneco, S.; Iiba, K.; Hiei, N.-H.; Ohta, K.; Mizuno, T.; Suzuki, T. *Electrochim. Acta* **1999**, *44*, 4701.
(16) Oh, Y.; Hu, X. *Chem. Commun.* **2015**, *51*, 13698.
(17) Hori, Y.; Murata, A.; Takahashi, R. *J. Chem. Soc., Faraday Trans. 1* **1989**, *85*, 2309.
(18) Murata, A.; Hori, Y. *Bull. Chem. Soc. Jpn.* **1991**, *64*, 123.
(19) Bumroongsakulsawat, P.; Kelsall, G. *Electrochim. Acta* **2014**, *141*, 216.
(20) Hori, Y.; Kikuchi, K.; Murata, A.; Suzuki, S. *Chem. Lett.* **1986**, *15*, 897.
(21) Paik, W.; Andersen, T.; Eyring, H. *Electrochim. Acta* **1969**, *14*, 1217.
(22) Singh, M. R.; Clark, E. L.; Bell, A. T. *Phys. Chem. Chem. Phys.* **2015**, *17*, 18924.
(23) Kyriacou, G.; Anagnostopoulos, A. *J. Appl. Electrochem.* **1993**, *23*, 483.
(24) Thorson, M. R.; Siil, K. I.; Kenis, P. J. *J. Electrochem. Soc.* **2013**, *160*, F69.
(25) Hori, Y.; Suzuki, S. *Bull. Chem. Soc. Jpn.* **1982**, *55*, 660.
(26) Frumkin, A. N. *Trans. Faraday Soc.* **1959**, *55*, 156.
(27) Mills, J.; McCrum, I.; Janik, M. *Phys. Chem. Chem. Phys.* **2014**, *16*, 13699.
(28) Strmcnik, D.; Kodama, K.; Van der Vliet, D.; Greeley, J.; Stamenkovic, V. R.; Marković, N. M. *Nat. Chem.* **2009**, *1*, 466.
(29) Kilic, M. S.; Bazant, M. Z.; Ajdari, A. *Phys. Rev. E* **2007**, *75*, 021502.
(30) Baes, C. F.; Mesmer, R. E. *Hydrolysis of Cations*; Wiley-Interscience: New York, 1976.
(31) Burgess, J. *Ions in Solution: Basic Principles of Chemical Interactions*, ed. II; Woodhead Publishing Limited: Cambridge, 1999.
(32) Kim, B.; Ma, S.; Jhong, H.-R. M.; Kenis, P. J. *Electrochim. Acta* **2015**, *166*, 271.
(33) Schizodimou, A.; Kyriacou, G. *Electrochim. Acta* **2012**, *78*, 171.

DOI: 10.1021/jacs.6b07612
J. Am. Chem. Soc. 2016, 138, 13006−13012